Supporting Information

for

"Thermal Transport in Quasi-1D van der Waals Crystal $Ta_2Pd_3Se_8$ Nanowires: Size and Length Dependence"

Qian Zhang,[1,†] Chenhan Liu,[2,†] Xue Liu,[3,†] Jinyu Liu,[3,†] Zhiguang Cui,[4] Yin Zhang,[1,2] Lin Yang,[1] Yang Zhao,[1] Terry T. Xu,[4] Yunfei Chen,[2] Jiang Wei,[3] Zhiqiang Mao,[3] and Deyu Li[1,]*

[1]*Department of Mechanical Engineering, Vanderbilt University, Nashville, TN 37235, USA*
[2]*School of Mechanical Engineering and Jiangsu Key Laboratory for Design and Manufacture of Micro-Nano Biomedical Instruments, Southeast University, Nanjing, 210096, P. R. China*
[3]*Department of Physics and Engineering Physics, Tulane University, New Orleans, LA 70118, United States*
[4]*Department of Mechanical Engineering and Engineering Science, The University of North Carolina at Charlotte, Charlotte, NC 28223, USA*

†: These authors contributed equally to this work

*: Author to whom correspondence should be addressed.

E-mail: deyu.li@vanderbilt.edu

Contents

I. Material Preparation

Single crystals of $Ta_2Pd_3Se_8$ (TPdS) were grown by chemical vapor transport (CVT) method. The growth condition can be found elsewhere.[1] Ta, Pd, and Se elements were mixed in stoichiometric ratio and thoroughly grounded before loading into a quartz tube. The tube was then sealed under vacuum and placed in a box furnace. Polycrystalline samples of TPdS are accessible by keeping the furnace at 750 ºC for one week. To grow single crystals, polycrystalline samples (~2 g) were ground and loaded into a new quartz tube (i.d. 9 mm) with iodine (75 mg) as transport agent. The vacuumed tube with a length of 15 cm was sealed and transferred to a double zone furnace. The temperatures at the charge end and "cold" end were then set to 850 ºC and 900 ºC, respectively, for one day before the temperatures were reversed. This process aims to eliminate any possible contamination in the "cold" end and keep a clean zone for the growth of single crystals. After growth for two weeks, TPdS would form needle-like single crystals with silver luster arranged in bundles at the cold end of the quartz tube.

The nanowire samples were prepared with a wet exfoliation method.[2] 0.5 mg bulk TPdS single crystal was immersed in 20 mL isopropanol alcohol (IPA) and then sonicated for 4 hours at 50 ºC with a total input power of 0.6 MJ. The mixture was turned into a stable TPdS nanowire suspension without significant re-aggregation after at least one week, which was then centrifuged at 500 rpm for 1 hour, and 2/3 of the supernatant was collected as the liquid form sample. The supernatant was then dropcasted onto a polydimethylsiloxane (PDMS) piece for subsequent manipulation and transport property measurements.

II. Contact Thermal Resistance Characterization

Electron beam induced deposition (EBID) of Platinum (Pt) was used to treat the contacts between individual nanowires and the suspended membranes. To confirm that we have reduced the contact thermal resistance to a negligible level, we employed a double bonding scheme,[3] which applied single bonding and double bonding to treat the contacts between the nanowires and the Pt electrodes underneath. Separate thermal measurements were conducted to confirm that the two separate runs, i.e., with single EBID bond and double EBID bonds on a nanowire of 80 nm in hydraulic diameter and 3.15 μm in suspended length (Figure S1a&b), produced the same results, with overlapping thermal conductance as shown in Figure S1c. This result confirms that the contact thermal resistance is reduced to a negligible level and the measured nanowire thermal conductivity is not affected by the contact thermal resistance.

III. Cross Section Characterization

The cross sections of the exfoliated nanowires are likely to be irregular. Therefore, it is imperative to characterize the cross section of each tested nanowire. We developed a method that directly exposes the cross sections for high-resolution SEM examination, which allows us to obtain the perimeter and cross-section of all measured samples. Acquisition of these quantities enables calculation of the hydraulic diameter of the corresponding nanowire.

Figure S2 illustrates the procedure. To begin, we placed the nanowire on the edge of a piece of pre-cut Si substrate, with the nanowire aligned in a perpendicular orientation to the edge

(Figure S2a). Then we applied EBID to deposit Pt to cover the nanowire, protecting the nanowire cross-section from being damaged in the subsequent focused ion beam cutting process (Figure S2b). Focused ion beam (FIB) was then employed to etch away part of the nanowire, cutting open the cross-section (Figure S2c). Finally, the prepared sample was mounted vertically on an SEM stub and loaded for direct visualization of the cross section (Figure S2d). Figure S2e shows the cross section of a nanowire that is covered by a thick layer of Pt-C deposits.

The acquisition of HRSEM images readily enable subsequent extraction of perimeter (P) and cross-sectional area (A) of the exposed cross sections, which then can be used to calculate the surface area to volume ratio (SVR) following equation SVR = P/A. The hydraulic diameter is calculated following $D_e = 4A/P$, that is, four times the reciprocal of the SVR.

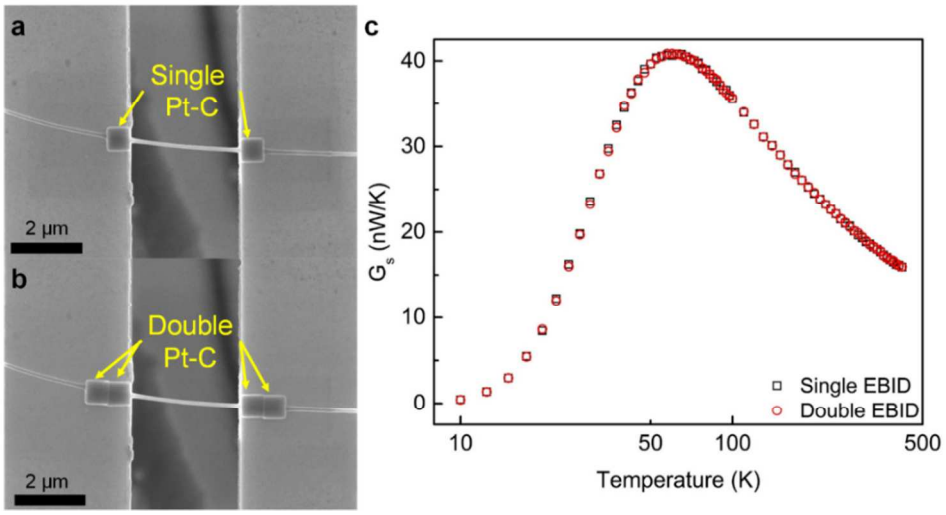

Figure S1. Contact thermal resistance characterization. SEM images showing the nanowire sample bonded by EBID Pt to the suspended membrane by (a) a single EBID treatment, and (b) double EBID treatments. (c) The measured thermal conductance of the nanowire sample before and after the second EBID treatment does not change, indicating that the contact thermal resistance is reduced to a negligible level by EBID treatment.

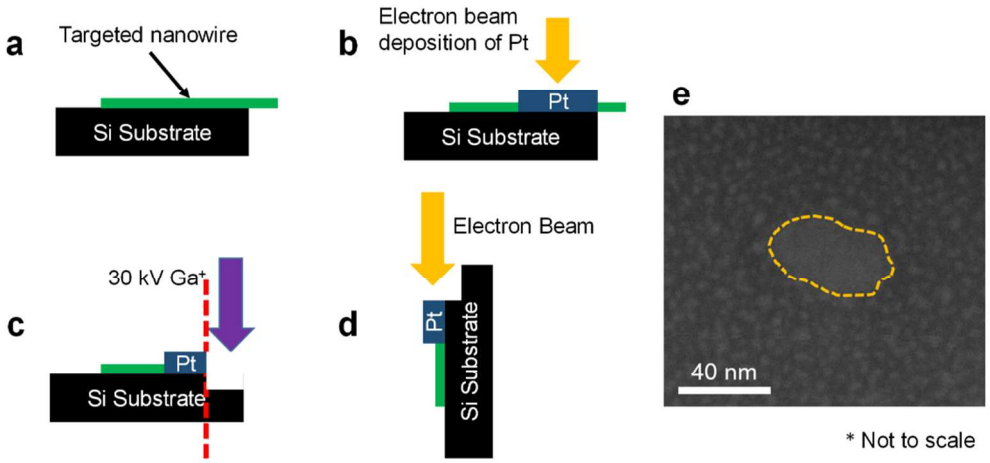

Figure S2. Cross-section examination. a) An individual nanowire was placed on the edge of a Si piece that has the edges well cut. b) EBID Pt was applied to cover the nanowire, preventing potential damage from the ion beam. c) Focused ion beam (FIB) was employed to remove part of the nanowire, exposing the cross section. d) The Si substrate was mounted vertically for direct SEM imaging of the cross section. e) A representative high-resolution SEM micrograph of the cross-section of a TPdS nanowire as outlined by the dashed yellow line.

IV. Ballistic Transport Length at 55 K and 300 K

As discussed in the main paper, the existence of the length dependence could hold up to 13 μm at 300 K due to partially ballistic phonon transport as indicated in Figure S3b. Such length dependence extends to an even longer distance at 17 μm at 55 K (peak temperature), due to weaker phonon-phonon scattering, which incurs much less disturbance to the ballistically transporting phonons as seen in Figure S3a.

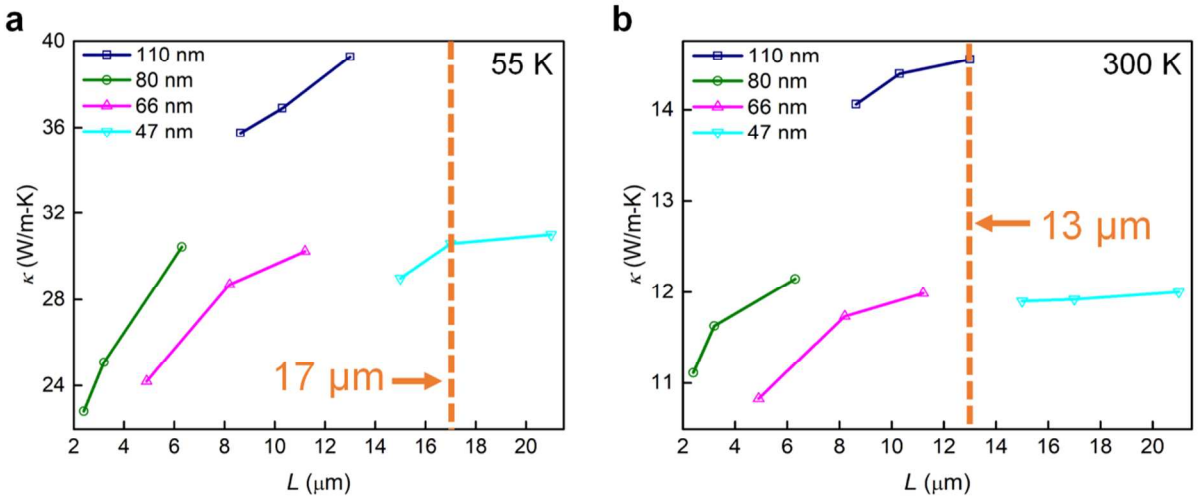

Figure S3. Length-dependent thermal conductivity for four samples of different hydraulic diameters at a) 55 K and b) 300 K.

V. First-principles Calculation

The Vienna Ab initio Simulation Package (VASP)[4] with projector-augmented-wave (PAW) pseudopotentials,[5] and Perdew–Burke–Ernzerhof (PBE) exchange and correlation functions[6] were used to relax the structure with force tolerance of 0.5×10^{-4} eV/Å. The $\boldsymbol{q}$ points were chosen as 4×6×12, similar to a recent calculation for TPdS.[1] The relaxed structure was used to calculate the elastic constants through the stress-strain relationship. The energy cutoff was carefully chosen to ensure that the results converged. Then the elastic constants were applied to calculate the iso-energy sufaces based on the Auld's theory.[7] Subsequently, a 2×2×3 supercell was employed to calculate the harmonic and anharmonic force constant of TPdS based on direct (finite displacement) method.

Using the harmonic force constants and the phonopy package,[8] we calculated the phonon dispersion. Using harmonic and anharmonic force constants acquired and a Boltzmann transport equation (BTE) package (ShengBTE),[9] we were able to calculate the thermal conductivity of TPdS. In the ShengBTE package, the phonon lifetimes are obtained using an iterative (full) solution of the linearized BTE and three-phonon interactions are considered to obtain the phonon-phonon scattering rates.

In order to verify the accuracy of elastic constants, the sound velocities obtained from elastic constants[7] and dispersion relations (group velocity at the Γ point) are compared. Table S1 indicates that they are very close, confirming that the calculation presented here is robust.

Table S1. The sound velocity of longitudinal acoustic (LA) branch phonon extracted from the phonon dispersion and elastic constant

	Dispersion	Elastic constant
V_x (m/s)	1863	2190
V_y (m/s)	2013	2028
V_z (m/s)	3867	3859

Under the framework of the BTE, the thermal conductivity tensor of TPdS at temperature T can be obtained as,[9]

$$k_{\alpha\beta} = \frac{1}{k_B T^2 \Omega N} \sum_\lambda f_0(f_0+1)(\hbar\omega)^2 v_\lambda^\alpha F_\lambda^\alpha, \quad \text{(S1)}$$

where k_B is the Boltzmann constant, N is number of unit cell, and Ω is the volume of unit cell, λ is the phonon mode with branch p and wave vector q, f_0 is the equilibrium Bose-Einstein distribution, $\hbar$ is the reduced Planck constant, ω is the phonon frequency, and υ is the group velocity. Here, F is written as

$$\vec{F} = \tau_\lambda^0 \left(\vec{v}_\lambda + \vec{\Delta}_\lambda\right), \quad \text{(S2)}$$

in which $\vec{\Delta}_\lambda$ is dependent on the $\vec{F}$, so $\vec{F}$ in Eq. (S2) has to be calculated iteratively. τ_λ^0 is the relaxation time of phonon mode λ, which is computed as

$$\frac{1}{\tau_\lambda^0} = \frac{1}{N}\left(\sum_{\lambda'\lambda''}^{+} \Gamma_{\lambda\lambda'\lambda''}^{+} + \frac{1}{2}\sum_{\lambda'\lambda''}^{-} \Gamma_{\lambda\lambda'\lambda''}^{-} + \sum_{\lambda'} \Gamma_{\lambda\lambda'}\right). \quad \text{(S3)}$$

In the three-phonon scattering process, the conservation of quasi-moment requires that $\vec{q}'' = \vec{q} \pm \vec{q}' + \vec{G}$ in the summation. Here the $\vec{G}$ is the reciprocal lattice vector, which allows $\vec{q}''$ to locate in the first Brillouin zone as $\vec{q}$ and $\vec{q}'$. The quantities $\Gamma_{\lambda\lambda'}$ describes the isotopic scattering rates and $\Gamma_{\lambda\lambda'\lambda''}^{\pm}$ describes the three-phonon scattering rates

$$\Gamma_{\lambda\lambda'\lambda''}^{+} = \frac{\hbar\pi(f_0' - f_0'')}{4\omega_\lambda\omega_{\lambda'}\omega_{\lambda''}} \left|V_{\lambda\lambda'\lambda''}^{+}\right|^2 \delta(\omega_\lambda + \omega_{\lambda'} - \omega_{\lambda''}) \quad \text{(S4)}$$

$$\Gamma_{\lambda\lambda'\lambda''}^{-} = \frac{\hbar\pi(f_0' + f_0'' + 1)}{4\omega_\lambda\omega_{\lambda'}\omega_{\lambda''}} \left|V_{\lambda\lambda'\lambda''}^{-}\right|^2 \delta(\omega_\lambda - \omega_{\lambda'} - \omega_{\lambda''}), \quad \text{(S5)}$$

respectively, where the delta function enables the energy conservation during the three-phonon scattering and $V^{\pm}_{\lambda\lambda'\lambda''}$ is the scattering matrix elements, which depends on the third-order force constants.[10] The above calculation procedure can be performed with the ShengBTE package,[9] which is the approach employed in this paper to calculate the thermal conductivity of TPdS.

Importantly, we point out that in TPdS the unit cell has 26 atoms, which is very time-consuming and memory-demanding to calculate. Therefore, in order to reduce the computation time and memory space, a 2×2×3 supercell (312 atoms) is adopted in the force constant calculation and 6×8×12 wave vectors are considered in the thermal conductivity calculation.

VI. References

1. Liu, X.; Liu, J.; Antipina, L. Y.; Hu, J.; Yue, C.; Sanchez, A. M.; Sorokin, P. B.; Mao, Z.; Wei, J. Direct Fabrication of Functional Ultrathin Single-Crystal Nanowires from Quasi-One-Dimensional van Der Waals Crystals. *Nano Lett.* **2016**, *16*, 6188–6195.
2. Coleman, J. N.; Lotya, M.; O'Neill, A.; Bergin, S. D.; King, P. J.; Khan, U.; Young, K.; Gaucher, A.; De, S.; Smith, R. J.; Shvets, I. V; Arora, S. K.; Stanton, G.; Kim, H.-Y.; Lee, K.; Kim, G. T.; Duesberg, G. S.; Hallam, T.; Boland, J. J.; Wang, J. J.; et al. Two-Dimensional Nanosheets Produced by Liquid Exfoliation of Layered Materials. *Science* **2011**, *331*, 568–571.
3. Hochbaum, A. I.; Chen, R.; Delgado, R. D.; Liang, W.; Garnett, E. C.; Najarian, M.; Majumdar, A.; Yang, P. Enhanced Thermoelectric Performance of Rough Silicon Nanowires. *Nature* **2008**, *451*, 163–167.
4. Kresse, G.; Furthmüller, J. Efficient Iterative Schemes for Ab Initio Total-Energy Calculations Using a Plane-Wave Basis Set. *Phys. Rev. B* **1996**, *54*, 11169–11186.
5. Blöchl, P. E. Projector Augmented-Wave Method. *Phys. Rev. B* **1994**, *50*, 17953–17979.
6. Perdew, J. P.; Burke, K.; Ernzerhof, M. Generalized Gradient Approximation Made Simple. *Phys. Rev. Lett.* **1996**, *77*, 3865–3868.
7. Auld, B. A. *Acoustic Fields and Waves in Solids*; John Wiley & Sons, Inc., 1973; pp 401-405.
8. Togo, A.; Tanaka, I. First Principles Phonon Calculations in Materials Science. *Scr. Mater.* **2015**, *108*, 1–5.
9. Li, W.; Carrete, J.; A. Katcho, N.; Mingo, N. ShengBTE: A Solver of the Boltzmann Transport Equation for Phonons. *Comput. Phys. Commun.* **2014**, *185*, 1747–1758.
10. Ward, A.; Broido, D. A.; Stewart, D. A.; Deinzer, G. Ab Initio Theory of the Lattice Thermal Conductivity in Diamond. *Phys. Rev. B* **2009**, *80*, 125203.